Astron. Astrophys. 322, 460–476 (1997)

ASTRONOMY
AND
ASTROPHYSICS

# Critical tests of stellar evolution in open clusters

## II. Membership, duplicity, and stellar and dynamical evolution in NGC 3680⋆,⋆⋆

**B. Nordström, J. Andersen, and M.I. Andersen**

Niels Bohr Institute for Astronomy, Physics, and Geophysics, Astronomical Observatory, Juliane Maries Vej 30, DK-2100 Copenhagen, Denmark

Received 2 October 1996 / Accepted 3 December 1996

**Abstract.** Based on new, accurate photometry, radial velocities, and proper motions for the intermediate-age open cluster NGC 3680, we identify individual single and binary cluster members and field stars in the colour-magnitude diagram (CMD). This basic step turns out to be crucial for a proper understanding of the cluster CMD: ∼60% of the stars are found to be field stars, and over 50% of the cluster stars are binaries. No *bona fide* cluster star is found more than $1\overset{\mathrm{m}}{.}5$ below the turnoff, and cluster stars below 1.4 $M_{\odot}$ are only found in binary systems. The total present mass of NGC 3680 is $\sim 100 M_{\odot}$, excluding any as yet unseen stellar remnants, and its half-mass radius is 3.3′ (1.2 pc). Comparison with plausible IMFs indicates that only ∼3% of the original stars and $\lesssim$10% of the mass now survive, ∼30% of the initial mass being in the form of massive stars that have now completed their evolution, and ∼60% in low-mass stars which may now be located in a distant cluster halo or perhaps have been lost entirely.

The single main-sequence cluster members form an extremely tight sequence in the CMD, with $E_{(b-y)}$ = 0.034 and [Fe/H] = +0.11. A direct fit to the Hyades main sequence yields $(m\text{-}M)_0$ = 10.5±0.2 for NGC 3680. Isochrones from several stellar models have been fit to the cluster sequence. When based on consistent *uvby* colour transformations and the above cluster parameters, these fits are very stable and show that standard models are not acceptable for stars with the turnoff mass of NGC 3680. Overshooting models perform much better, but further refinement of the overshooting formalism seems to be needed. The age derived for NGC 3680 is 1.45±0.3 Gyr. The limiting factor in a precise comparison of theory and observations is now the transformation from theoretical to observed parameters, particularly (broad-band) colours.

**Key words:** stars: evolution; fundamental parameters; HR diagram; kinematics; luminosity function, mass function – open clusters and associations: NGC 3680

*Send offprint requests to*: B. Nordström (birgitta@astro.ku.dk)

⋆ Based on observations obtained with the Danish 1.5-m telescope at the European Southern Observatory, La Silla, Chile.

⋆⋆ Table 1 is available in electronic form at the CDS via anonymous ftp to 130.79.128.5.

### 1. Introduction

Star clusters are classic research tools in stellar and Galactic astronomy (see Friel 1995 for a recent review). Their use in the determination of distances, ages, and metal abundances of Galactic populations and their gradients is well known (e.g. Friel & Janes 1993, Janes & Phelps 1994). Equally importantly, as ensembles of stars of identical age and chemical composition, star clusters are favourite test objects for stellar evolution models (e.g. VandenBerg 1983, 1985 and numerous later papers). Moreover, our knowledge of key properties of certain rare stellar types (e.g. Cepheids, blue stragglers, various peculiar stars) derives from the cluster membership of specimens of such stars. In view of the current vigorous development of increasingly sophisticated stellar evolution models, improving the quality of test and calibration data from clusters becomes a matter of priority.

CCD detectors and modern reduction software have been crucial ingredients in the large number of precise photometric studies of open and globular cluster CMDs in recent years. Examples are, e.g., the high-precision studies of M67 by Gilliland et al. (1991) or the recent spectacular results from the refurbished *Hubble Space Telescope* (Paresce et al. 1995, von Hippel et al. 1996). No doubt, the quality and quantity of cluster CMDs will continue to improve over the next several years. High internal precision is not enough, however; careful standardisation and calibration of the photometric system are essential. Moreover, especially in critical tests of stellar evolution models, precise observational determinations of reddening and metal abundance are needed to minimize the number of adjustable parameters when fitting models to the CMD.

Finally, most applications of cluster CMDs implicitly assume that a sequence of single cluster stars can be defined. Real CMDs, however, also contain field and binary stars which complicate the interpretation, especially in open clusters if the contrast from the background of field stars is low and binary stars are frequent. Accurate proper-motion are important tools, but still exist only for a handful of nearby clusters and leave close binaries undetected. In contrast, precise radial velocities provide information on both cluster membership and duplic-

ity and can be readily obtained. A textbook case is the Hyades moving cluster (Schwan 1991), but radial-velocity data have also proved valuable in, e.g. the classic cluster M67 (Mathieu et al. 1986; Nissen et al. 1987) or the younger NGC 752 (Daniel et al. 1994). This paper discusses the first results of a program to provide such precise radial-velocity data for southern open clusters.

The intermediate-age NGC 3680 was selected as the first cluster in this program, for two main reasons:

First, NGC 3680 has been repeatedly cited as evidence both in favour of (Anthony-Twarog et al. 1991, AHTC; Carraro et al. 1993) and against (Castellani et al. 1992) the significance of convective core overshooting in stars in this mass and age range, based on the CMDs of Anthony-Twarog et al. 1989 (ATTS) and AHTC. While it has appeared in the meantime that the large ages derived from some early overshooting models were of numerical rather than astrophysical origin, the true shape of cluster turnoffs remains a key observational constraint on convection prescriptions for models of intermediate-mass stars.

Second, the putative phenomenon of a "bimodal" or "bifurcated" main-sequence turnoff, first noted in NGC 752 by Twarog (1983), has been extensively discussed also for NGC 3680 by ATTS and Nissen (1988, N88). While canonical stellar evolution theory predicts no such phenomenon, none of the more prosaic alternative interpretations carefully discussed in N88 appeared fully convincing either. Hence, it appeared worthwhile to re-examine the observational basis for this result.

Finally, as our study was under way, AHTC called attention to a further unusual feature of NGC 3680, shared with its two sister clusters NGC 752 (Daniel et al. 1994) and IC 4651 (Anthony-Twarog & Twarog 1987; Anthony-Twarog et al. 1988), i.e. the marked deficiency of stars on the lower main sequence. We therefore extended our radial-velocity survey to include all observable main-sequence candidates in the AHTC field.

It became clear fairly early (Andersen et al. 1990, Andersen & Nordström 1991, Nordström & Andersen 1991) that the impact of the binaries and non-members in NGC 3680 is so strong that trustworthy model fits must be based on detailed, individual membership and duplicity data, a simple message that was perhaps somewhat overshadowed by our secondary conclusion that the real main sequence seemed to agree best with the predictions of overshooting models. Both conclusions are strongly reinforced by the extreme nature of NGC 3680 as uncovered in the present detailed analysis of our new photometric and radial-velocity data (Nordström et al. 1996; Paper I).

In the following, we review the basic observational data for NGC 3680 (photometry, radial velocities, proper motions) in Sect. 2, and use them in Sect. 3 to define the subsets of single and binary cluster members, study their spatial, radial and rotational velocity distributions, and compute the mean reddening, metal abundance, and distance of the cluster. Sect. 4 reviews the main current sets of stellar evolution models applicable to NGC 3680 and the corresponding transformations from theoretical to observational quantities, examines the fit of standard and overshooting isochrones to the CMD, and uses the best-fit isochrone to estimate the masses of all cluster stars. In Sect. 5 we estimate the total initial mass of the cluster and discuss its dynamical evolution, the constraints on stellar evolution models provided by NGC 3680, and its age. Finally, our conclusions are summarised in Sect. 6.

## 2. Basic observational data for NGC 3680

The observational history of NGC 3680 is reviewed in detail in Paper I. Briefly, following the early photoelectric $UBV$ photometry of 79 stars in and near NGC 3680 by Eggen (1969), photoelectric *uvby-*$H_\beta$ photometry for 33 stars was presented by N88 and deeper CCD $uvby$ photometry for the centre of the cluster by ATTS. Photoelectrically calibrated photographic $BV$ photometry for ∼500 stars to a limit of $V$ = 17.6 in a large field ($20' \times 20'$) around the cluster was published by AHTC and remains the most complete source for outlying cluster members.

Subsequently, in Paper I we presented CCD $by$ photometry of high precision for 310 stars to $V$ = 18 in a $13' \times 13'$ field centered on NGC 3680 (note that the first page of Table 1 is unfortunately missing in the printed, but not in the electronic version of Paper I). Paper I also gives mean radial velocities for a total of 109 stars in the AHTC field, based on ∼400 individual CORAVEL observations covering a baseline of typically six years for the main-sequence stars and ten years for the red giants; for the giants, the detailed data were published by Mermilliod et al. (1995). Rotational velocities were also determined from the CORAVEL cross-correlation profiles. Finally, a proper-motion study of NGC 3680 was published by Kozhurina-Platais et al. (1995; K95).

Extensive cross-checking and consistency analysis was carried out on these data in Paper I, to which the reader is referred for further details. The following salient results are important for the discussion in the present paper:

First, a unified numbering system for the stars in the field of NGC 3680 was derived from the several previous systems, such that numbers below 100 refer to Eggen (1969), between 1000 and 5000 to AHTC, between 6000 and 8000 to ATTS (subtract 4000 to get ATTS numbers as published), and numbers above 9000 to stars newly observed in our CCD photometry. This system is used throughout in the following. Accurate J2000 coordinates and K95 numbers are also given in Paper I.

Second, the photometric zero-points and scales of the published (photoelectric and photographic) $BV$ photometry were found to suffer from appreciable random and systematic errors. A correction formula for the AHTC *(B-V)* data was given, based on a re-examination of the original data by Drs. Twarog and Anthony-Twarog, but significant uncertainties remain. The CCD $uvby$ data of ATTS and Paper I were all calibrated with the photoelectric data by N88 and are in much better agreement, but do not cover as large a field as AHTC. Comments are given in Paper I on large discrepancies for several individual stars. Our discussion below of the CMD of NGC 3680 will be based primarily on the new CCD $by$ data from Paper I; when stars in the outer field need to be plotted, the corrected AHTC data will be used.

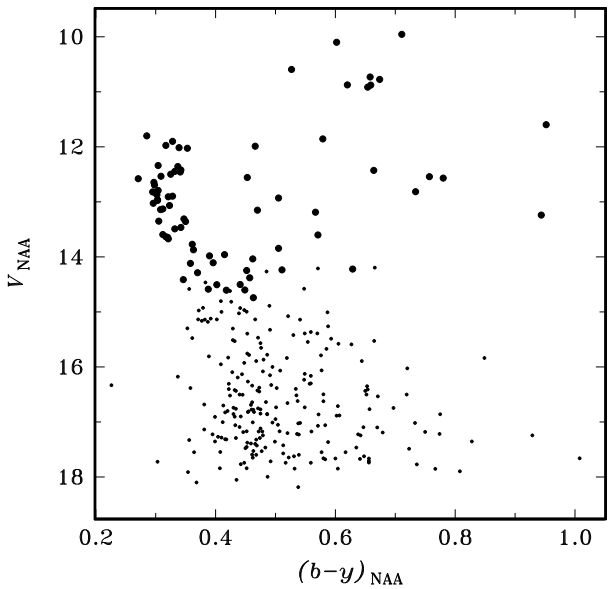


**Fig. 1.** CMD of NGC 3680 from the *by* photometry of Paper I; large symbols show the stars with CORAVEL observations

Third, the consistency of the new CORAVEL radial velocities was examined as a function of stellar rotation, and a procedure was developed to refine the internal error estimates for fast-rotating stars ($v \sin i > 15$ km s$^{-1}$). On this basis, a velocity variability criterion was defined, and single stars and certain or probable binaries were identified. The coordinates, mean radial and rotational velocities and new *by* CCD photometry for these 109 stars, and the binary identifications, are the main observational basis for the following analysis. Fig 1 shows the new *(b-y)* CMD, highlighting stars with radial-velocity observations.

For reference in the present paper, Table 1 lists the numbers of the stars observed with CORAVEL, $V$ magnitudes and *(b-y)* colours from Paper I for stars in the CCD field ($V$ magnitudes are from AHTC for stars in the outer field), *(B-V)* colours from AHTC, corrected as described in Paper 1, mean radial velocities and mean errors from Paper I, radial-velocity membership probabilities as derived below, proper-motion membership probabilities from K95, and the resulting classification of the stars into members (MB) and non-members (NM) and single stars or binaries (SB1, SB2). SB1O denotes a published binary orbit (Mermilliod et al. 1995).

## 3. Present properties of NGC 3680

### *3.1. Identification of cluster members*

#### 3.1.1. Radial-velocity membership criterion

Agreement of an accurate radial velocity with the cluster mean is one of the best objective indicators of cluster membership for a given star. Accurate proper motions like those by K95 can also be used to assign individual membership probabilities, based on proper motions alone as well as on a combination of proper motion and spatial distribution, but the mean proper motion of NGC 3680 is not much different from that of the field. Distance from the cluster centre alone is an ineffective criterion in a loose cluster like NGC 3680, with poorly-defined borders. Finally, the "photometric" method of assigning cluster membership from position in the CMD assumes some $a\ priori$ knowledge of the precise shape of the cluster sequence - the very feature we wish to determine.

The overall contrast of cluster vs. field in velocity space was shown in Paper I (Fig. 9). A constant-velocity cluster star may deviate from the precise cluster mean velocity for three main reasons: *(i)* Observational error; *(ii)* intrinsic velocity dispersion in the cluster; and *(iii)* undetected motion in a long-period binary orbit. We define an objective, quantitative diagnostic of the significance of the observed velocity residuals, usable to derive meaningful membership probabilities, as follows:

The mean radial velocity $V_{cl}$ (+0.87 km s$^{-1}$) and velocity dispersion $\sigma_{cl}$ (0.35 km s$^{-1}$) of NGC 3680 were determined by Mermilliod et al. (1995) from the six sharp-lined constant-velocity cluster giants. Subtracting the average observational error of 0.12 km s$^{-1}$ for the individual giants leaves $\sigma_{cl}$ = 0.33 km s$^{-1}$ as our best estimate of the true velocity dispersion of NGC 3680.

For a population of constant-velocity cluster stars with observational error $\sigma_{obs}$, the predicted standard deviation of the individual velocities from $V_{cl}$ is the quadratic sum of $\sigma_{obs}$ and the intrinsic velocity dispersion of the cluster:

$$\chi^2 = (V_{obs} - V_{cl})^2/(\sigma^2_{obs} + \sigma^2_{cl}) \quad (1)$$

Thus, we can use the cumulative $\chi^2$ distribution function $P(\chi^2)$ with one degree of freedom to derive the radial-velocity membership probability $P(RV)$. Consistent with our adopted 99% confidence level for detection of binaries, stars with $P(RV) > 0.01$ will be considered to be cluster members, stars with $P(RV) < 0.005$ to be definite non-members, and stars with $0.005 < P(RV) < 0.01$ to be marginal cases. Thus, we require the velocity residuals to be highly significant before rejecting the default hypothesis of membership or non-variability.

To our initial surprise, the mean radial velocity of the main-sequence cluster members so defined was about 1.32 km s$^{-1}$, significantly larger than $V_{cl}$ as derived from the red giants (see Fig. 2). In fact, this is to be expected since the fixed spectral mask in CORAVEL makes no allowance for the change in gravitational redshift between the main-sequence F dwarfs and the giants. In velocity units, the gravitational redshift is:

$$RV_g = 0.64\ (M/R) \text{ km s}^{-1} \quad (2)$$

($M$ and $R$ in solar units). Data for well-studied binary stars similar to those in NGC 3680 (Andersen 1991) indicate that $M/R \approx 0.9$ for the F dwarfs and $\approx$0.2 for the giants. Hence, the average dwarf velocities should be about 0.40 km s$^{-1}$ larger than those of the giants, exactly as observed. Since radial-velocity zero-points are ultimately calibrated to yield correct results for solar-system objects, i.e. for (reflected) sunlight, we adopt the

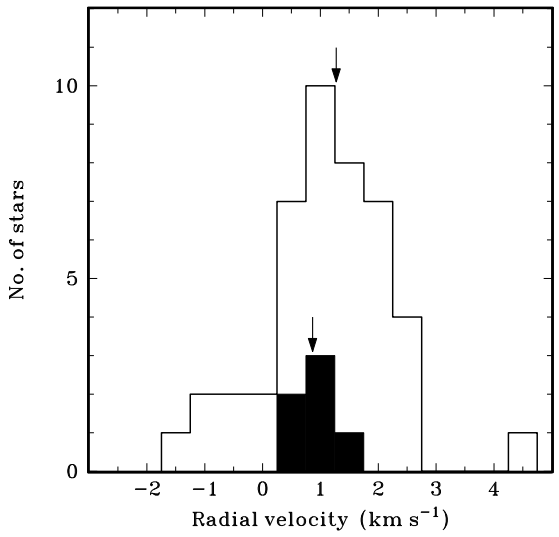


**Fig. 2.** Velocity histogram for the radial-velocity members of NGC 3680. Open curve: All member stars; solid: single giant members only. Arrows show the mean velocity of each group

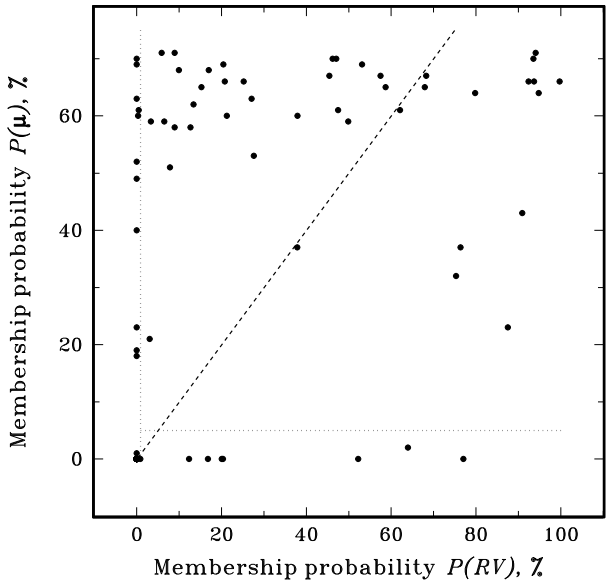


**Fig. 3.** Radial-velocity vs. proper-motion membership probabilities for the stars in Table 1. Dotted lines show the limits for membership; the dashed line is the relation $P(RV) = P(\mu)$

dwarf value $V_{cl}$ = +1.27 km s$^{-1}$ as our best estimate for the centre-of-mass velocity of NGC 3680.

Accordingly, we recalculated $P(RV)$ for the dwarfs, assuming $V_{cl}$ = +1.27 km s$^{-1}$ (Eq. 1); thus, $P(RV)$ as given in Table 1 for dwarfs and giants refers to the appropriate (and different) values of $V_{cl}$. The resulting list of cluster members is affected negligibly by this revision, and the mean velocity of the constant cluster dwarfs changes by only 0.01 km s$^{-1}$; thus, we adopt these radial-velocity membership probabilities as final.

The standard deviation from $V_{cl}$ is 1.05 km s$^{-1}$ for the single dwarfs, or about 0.65 km s$^{-1}$ after subtraction of the mean observational error of 0.90 km s$^{-1}$, somewhat larger than found for the giants. Not too surprisingly, given the limited number, time span and precision of the dwarf radial velocities (broad, shallow CORAVEL profiles), a few low-amplitude binaries thus seem to remain in the sample. Conversely, a few stars now classified as single field stars from small, but significant velocity residuals might turn out to be long-period cluster binaries if observed long enough; star 3001, close to the cluster both on the sky and in the CMD, might be such a case.

Membership probabilities for spectroscopic binaries (SB1 and SB2) are computed as for single stars, but are somewhat less rigorously defined since precise systemic velocities are generally not available.

### 3.1.2. Combined membership criteria and final membership list

Our radial-velocity membership probabilities ($P(RV)$) and the K95 proper-motion probabilities ($P(\mu)$) are given in Table 1. In principle, they should define the same samples of member and field stars. In practice, both have uncertainties due to observational errors, especially for the fainter stars, and to unrecognised binaries.

$P(\mu)$ and $P(RV)$ are compared in Fig. 3. Since $P(\mu) < 5\%$ was adopted by K95 and $P(RV) < 1\%$ by us as the limits for certain non-membership, most of Fig. 3 contains stars that *could* (but not *must*) be members of NGC 3680, while all unambiguous field stars are concentrated in the single point $P(\mu) = P(RV) = 0$. Generally, we will consider a star to be a cluster member if it is within the field of the CCD photometry of Paper I and satisfies both of the criteria defined above. We note that, since these criteria are chosen to retain a maximum of true cluster members, a few field stars will tend to be included as well.

Our final results are given in the column labelled "Membership" in Table 1, and Fig. 4 shows the distribution of field stars and single and binary cluster members in the *by* CMD of NGC 3680. A few main features stand out: The large population of field stars; the near-total absence of faint main-sequence members, E70 (I) being the only certified single main-sequence member more than $1\overset{m}{.}5$ below the tip of the turnoff; the tightly defined sequence of single main-sequence cluster stars; and the prominent sequence of cluster binaries above the main sequence and to the blue of the red-giant clump.

A few *bona fide* single cluster members as defined by the above criteria still appear outside the main cluster locus (E4, 35, 45). The low velocity contrast of NGC 3680 from the field makes it easier for a couple of random field stars to fall inside our cluster limits, and we do note that the average distance moduli of E4 and E35 from N88 are ∼0.5 mag smaller than the cluster mean. The possibility also exists that the three stars may be long-period and/or low-inclination binaries; e.g., the central giant E34 is an obvious member with constant velocity, yet is clearly a binary as judged from the photometry and CORAVEL profile. In the following, we include the three stars in our membership

**Table 1.** Summary data for stars in the field of NGC 3680. $V$ is from Paper I for stars with measured *(b-y)*, otherwise from AHTC; their *(B-V)* has been corrected as described in Paper 1. Mean radial velocities and errors (km $s^{-1}$) are from Paper 1, $P(RV)$ was computed in Sect. 3.1.1, and $P(\mu)$ is from K95 (both in percent). Final membership assignment is given in the last column

| No. | $V$ | *(b-y)* | $(B\text{-}V)_c$ | $< RV >$ | m.e. | $P(RV)$ | $P(\mu)$ | Membership | |
|---|---|---|---|---|---|---|---|---|---|
| 1 | 11.922 | | 0.481 | -4.96 | 2.10 | 0.3 | 60 | SB2 | NM |
| 2 | 14.605 | 0.418 | 0.713 | -8.27 | 0.31 | 0.0 | 0 | | NM |
| 3 | 11.625 | | 0.541 | 11.86 | 0.36 | 0.0 | 0 | | NM |
| 4 | 12.897 | 0.328 | 0.531 | 0.91 | 0.63 | 62.1 | 61 | | MB |
| 5 | 12.830 | 0.299 | 0.477 | -1.50 | 6.76 | 68.3 | 67 | SB1 | MB |
| 6 | 12.458 | 0.341 | 0.550 | 0.37 | 0.52 | 15.3 | 65 | | MB |
| 7 | 13.241 | 0.944 | 1.572 | 57.67 | 1.05 | 0.0 | 19 | SB1 | NM |
| 8 | 12.570 | 0.780 | 1.347 | 9.40 | 0.23 | 0.0 | 0 | | NM |
| 9 | 14.120 | 0.358 | 0.583 | 2.59 | 0.50 | 3.1 | 21 | SB1 | MB |
| 10 | 12.822 | 0.295 | 0.456 | -1.01 | 1.16 | 5.9 | 71 | | MB |
| 11 | 10.878 | 0.620 | 1.035 | -0.27 | 0.20 | 0.5 | 61 | SB1 | MB |
| 13 | 10.776 | 0.674 | 1.135 | 0.90 | 0.12 | 93.5 | 70 | | MB |
| 14 | 12.340 | 0.304 | 0.491 | 0.83 | 0.73 | 58.7 | 65 | SB2 | MB |
| 15 | 12.499 | 0.325 | 0.519 | 1.93 | 0.38 | 20.4 | 69 | | MB |
| 16 | 13.312 | 0.347 | 0.583 | 37.87 | 7.11 | 0.0 | 63 | SB2 | NM |
| 17 | 11.600 | 0.952 | 1.593 | 31.46 | 0.19 | 0.0 | 0 | | NM |
| 18 | 11.992 | 0.466 | 0.791 | -2.34 | 0.07 | 0.0 | 0 | SB1O | NM |
| 19 | 12.360 | 0.337 | 0.536 | 0.41 | 1.14 | 47.1 | 70 | | MB |
| 20 | 10.102 | 0.602 | 0.945 | 0.62 | 0.13 | 49.9 | 59 | SB2 | MB |
| 21 | 14.507 | 0.402 | 0.643 | 11.04 | 0.36 | 0.0 | 0 | | NM |
| 21A | 14.744 | 0.463 | | 1.58 | 0.57 | 63.9 | 2 | SB2 | MB? |
| 22 | 13.358 | 0.350 | 0.553 | 1.32 | 0.26 | 90.9 | 43 | SB1 | MB |
| 23 | 13.982 | 0.390 | 0.629 | 0.67 | 0.58 | 37.9 | 60 | SB1 | MB |
| 24 | 13.773 | 0.361 | 0.574 | 2.44 | 0.57 | 7.9 | 51 | SB1 | MB |
| 25 | 13.673 | 0.321 | 0.501 | 2.15 | 0.61 | 20.8 | 66 | SB1 | MB |
| 25A | 13.646 | 0.320 | 0.495 | -0.75 | 1.04 | 6.5 | 59 | | MB |
| 26 | 10.915 | 0.654 | 1.098 | 0.32 | 0.11 | 13.4 | 62 | | MB |
| 27 | 10.734 | 0.658 | 1.163 | 0.83 | 0.46 | 94.1 | 71 | SB1O | MB |
| 29 | 11.974 | 0.317 | 0.512 | 3.44 | 0.18 | 0.0 | 0 | | NM |
| 30 | 13.597 | 0.312 | | 1.57 | 0.90 | 75.3 | 32 | | MB |
| 31 | 13.129 | 0.312 | 0.478 | 8.24 | 1.01 | 0.0 | 69 | SB1 | NM |
| 32 | 12.909 | 0.321 | 0.499 | 1.37 | 0.98 | 92.4 | 66 | SB1 | MB |
| 33 | 11.902 | 0.328 | 0.515 | -0.93 | 1.89 | 25.2 | 66 | SB1 | MB |
| 34 | 10.596 | 0.527 | 0.842 | 1.29 | 0.15 | 27.1 | 63 | Bin? | MB |
| 35 | 13.068 | 0.323 | 0.503 | 0.61 | 0.33 | 17.0 | 68 | | MB |
| 36 | 13.466 | 0.342 | 0.539 | 1.12 | 0.47 | 79.8 | 64 | SB2 | MB |
| 37 | 13.026 | 0.296 | 0.444 | 2.18 | 0.76 | 27.6 | 53 | | MB |
| 38 | 12.447 | 0.332 | 0.543 | 1.11 | 2.02 | 93.7 | 66 | SB1 | MB |
| 39 | 12.423 | 0.342 | 0.537 | 1.27 | 0.41 | 99.7 | 66 | | MB |
| 40 | 12.428 | 0.664 | 1.143 | -15.26 | 0.19 | 0.0 | 0 | | NM |
| 41 | 10.880 | 0.659 | 1.159 | 0.93 | 0.13 | 87.5 | 23 | | MB |
| 42 | 12.963 | 0.303 | 0.427 | | | | 62 | | MB? |
| 43 | 12.535 | 0.309 | 0.464 | 2.71 | 0.80 | 10.0 | 68 | | MB |
| 44 | 9.957 | 0.711 | 1.224 | 1.15 | 0.10 | 45.4 | 67 | | MB |
| 45 | 12.018 | 0.339 | 0.532 | 1.60 | 0.48 | 57.5 | 67 | | MB |
| 46 | 13.352 | 0.305 | 0.452 | 2.00 | 0.46 | 21.3 | 60 | | MB |
| 46A | 13.493 | 0.332 | 0.492 | 7.43 | 1.64 | 0.0 | 49 | | NM |
| 48 | 11.802 | 0.285 | 0.427 | -14.02 | 3.22 | 0.0 | 1 | | NM |
| 49 | 12.932 | 0.505 | 0.830 | 67.45 | 9.37 | 0.0 | 0 | | NM |
| 50 | 11.897 | | 0.815 | 50.70 | 0.18 | 0.0 | 0 | | NM |
| 53 | 10.796 | | 1.139 | 0.64 | 0.12 | 53.1 | 69 | | MB |
| 54 | 8.920 | | 1.122 | 16.54 | 0.50 | 0.0 | 0 | SB1 | NM |
| 55 | 11.823 | | 0.806 | | | | 0 | | NM |

**Table 1.** (continued)

| No. | $V$ | *(b-y)* | $(B\text{-}V)_c$ | $< RV >$ | m.e. | $P(RV)$ | $P(\mu)$ | Membership | |
|---|---|---|---|---|---|---|---|---|---|
| 57 | 12.582 | 0.271 | 0.430 | 33.85 | 4.04 | 0.0 | 0 | | NM |
| 58 | 12.874 | 0.302 | 0.457 | 34.01 | 19.28 | 9.0 | 58 | SB1 | MB |
| 59 | 12.544 | 0.757 | 1.211 | -13.67 | 0.26 | 0.0 | 0 | | NM |
| 60 | 14.290 | | 0.641 | 1.92 | 0.24 | 12.7 | 58 | | MB? |
| 61 | 14.414 | | 0.818 | 12.08 | 0.58 | 0.0 | 0 | SB1 | NM |
| 62(A) | 9.847 | | 0.461 | 4.36 | 2.21 | 16.8 | 0 | SB2 | NM |
| 63(B) | 11.594 | | 1.282 | -20.81 | 0.17 | 0.0 | 0 | | NM |
| 64(C) | 12.275 | | 0.925 | -6.85 | 6.37 | 20.4 | 0 | SB1 | NM |
| 65(D) | 13.168 | | 0.546 | 18.13 | 0.56 | 0.0 | 0 | | NM |
| 66(E) | 11.761 | | 0.563 | 32.16 | 2.83 | 0.0 | 0 | SB1 | NM |
| 67(F) | 12.817 | | 0.578 | -0.31 | 0.32 | 0.1 | 0 | | NM |
| 68(G) | 13.218 | | 0.584 | 15.29 | 0.35 | 0.0 | 0 | | NM |
| 69(H) | 14.296 | | 0.864 | | | | 0 | | NM |
| 70(I) | 14.589 | 0.388 | 0.651 | 1.41 | 0.30 | 76.4 | 37 | | MB |
| 71(J) | 12.558 | 0.453 | 0.777 | 6.71 | 0.22 | 0.0 | 0 | | NM |
| 72(K) | 12.696 | 0.298 | 0.463 | | | | 58 | | MB? |
| 74(N) | 12.974 | 0.303 | 0.479 | 1.41 | 0.32 | 77.0 | 0 | | NM |
| 76(P) | 12.376 | | 1.241 | 36.89 | 0.16 | 0.0 | 0 | | NM |
| 77(Q) | 13.101 | | 0.502 | -7.24 | 0.46 | 0.0 | 0 | | NM |
| 78(R) | 11.844 | | 0.494 | | | | 51 | | MB? |
| 1043 | 14.239 | 0.511 | 0.864 | | | | 0 | | NM |
| 1079 | 13.954 | | 0.578 | 10.73 | 0.76 | 0.0 | 0 | | NM |
| 1083 | 14.156 | | 0.626 | 3.52 | 0.41 | 0.0 | 0 | | NM |
| 1085 | 14.290 | 0.370 | 0.571 | 0.87 | 0.52 | 52.2 | 0 | | NM |
| 1092 | 13.151 | 0.470 | 0.769 | 7.01 | 0.27 | 0.0 | 0 | | NM |
| 1094 | 14.248 | 0.452 | 0.797 | | | | 0 | | NM |
| 1124 | 14.296 | | 0.564 | | | | 51 | | MB? |
| 2030 | 14.602 | 0.449 | 0.747 | | | | 0 | | NM |
| 2032 | 13.604 | 0.571 | 1.038 | -14.32 | 0.54 | 0.0 | 0 | | NM |
| 2040 | 14.626 | | 0.645 | -15.84 | 0.51 | 0.0 | 0 | | NM |
| 2062 | 13.637 | 0.317 | 0.463 | 1.98 | 0.94 | 47.5 | 61 | SB1 | MB |
| 2076 | 13.138 | | 1.159 | 56.65 | 0.65 | 0.0 | 0 | | NM |
| 2085 | 14.037 | 0.462 | 0.745 | -1.39 | 0.25 | 0.0 | 0 | | NM |
| 2093 | 13.872 | 0.363 | 0.543 | -10.51 | 1.84 | 0.0 | 0 | SB1 | NM |
| 2094 | 14.316 | | 0.664 | -7.21 | 6.62 | 20.0 | 0 | SB1 | NM |
| 2095 | 14.415 | 0.346 | 0.573 | 9.11 | 0.66 | 0.0 | 0 | | NM |
| 2096 | 14.382 | 0.457 | 0.802 | -1.86 | 0.38 | 0.0 | 0 | | NM |
| 2098 | 12.816 | 0.734 | 1.230 | 32.29 | 0.35 | 0.0 | 0 | | NM |
| 2110 | 12.612 | | 0.470 | | | | 57 | | MB? |
| 2117 | 11.769 | | 1.163 | -22.12 | 0.30 | 0.0 | 23 | | NM |
| 2118 | 13.105 | | 0.549 | 0.59 | 0.26 | 12.4 | 0 | | NM |
| 2125 | 13.031 | | 0.485 | 12.06 | 0.58 | 0.0 | 0 | | NM |
| 3001 | 12.796 | 0.304 | 0.459 | 3.62 | 0.41 | 0.0 | 70 | | NM |
| 3022 | 14.224 | 0.629 | 1.087 | -40.80 | 0.57 | 0.0 | 18 | | NM |
| 3028 | 13.865 | | 0.733 | 52.49 | 0.60 | 0.0 | 0 | | NM |
| 3040 | 13.803 | | 1.072 | 23.59 | 0.65 | 0.0 | 0 | | NM |
| 3064 | 14.108 | 0.396 | 0.661 | -22.10 | 1.06 | 0.0 | 52 | | NM |
| 3095 | 12.318 | | 0.529 | 1.07 | 2.99 | 94.8 | 64 | | MB? |
| 3104 | 12.300 | | 1.572 | 56.65 | 0.25 | 0.0 | 40 | | NM |
| 3105 | 14.342 | | 0.598 | 6.00 | 0.49 | 0.0 | 0 | | NM |
| 3113 | 13.060 | | 1.403 | 124.39 | 0.51 | 0.0 | 0 | | NM |
| 4002 | 13.141 | 0.308 | 0.444 | 0.16 | 1.47 | 46.2 | 70 | SB1 | MB |
| 4011 | 14.503 | 0.441 | 0.760 | 63.06 | 0.50 | 0.0 | 0 | | NM |
| 4015 | 13.188 | 0.567 | 1.050 | 25.86 | 0.30 | 0.0 | 0 | | NM |
| 4027 | 13.146 | | 0.773 | -15.57 | 0.40 | 0.0 | 0 | | NM |

**Table 1.** (continued)

| No. | $V$ | *(b-y)* | $(B\text{-}V)_c$ | $< RV >$ | m.e. | $P(RV)$ | $P(\mu)$ | Membership | |
|---|---|---|---|---|---|---|---|---|---|
| 4028 | 12.700 | | 0.463 | 0.96 | 0.65 | 67.9 | 65 | | MB? |
| 4081 | 12.411 | | 0.527 | -0.08 | 0.71 | 9.0 | 71 | SB1 | MB? |
| 4088 | 13.846 | 0.505 | 0.905 | 9.49 | 0.35 | 0.0 | 0 | | NM |
| 4094 | 11.858 | 0.579 | 1.021 | -0.18 | 0.19 | 0.8 | 0 | | NM |
| 4106 | 12.210 | | 0.526 | -9.68 | 0.51 | 0.0 | 0 | | NM |
| 4114 | 14.006 | | 0.634 | 1.78 | 0.47 | 37.9 | 37 | | MB? |
| 4116 | 13.959 | 0.415 | 0.716 | 33.25 | 0.61 | 0.0 | 0 | | NM |
| 4121 | 13.560 | | 0.556 | 4.56 | 1.51 | 3.3 | 59 | SB? | MB? |
| 4140 | 13.454 | | 0.914 | 17.63 | 0.84 | 0.0 | 0 | | NM |
| 6027 | 12.026 | 0.353 | | | | | | | |
| 6028 | 12.648 | 0.297 | | 2.29 | 0.20 | 1.2 | | SB2 | MB? |
| 7020 | 14.266 | 0.485 | | 48.30 | 0.40 | 0.0 | | | NM |

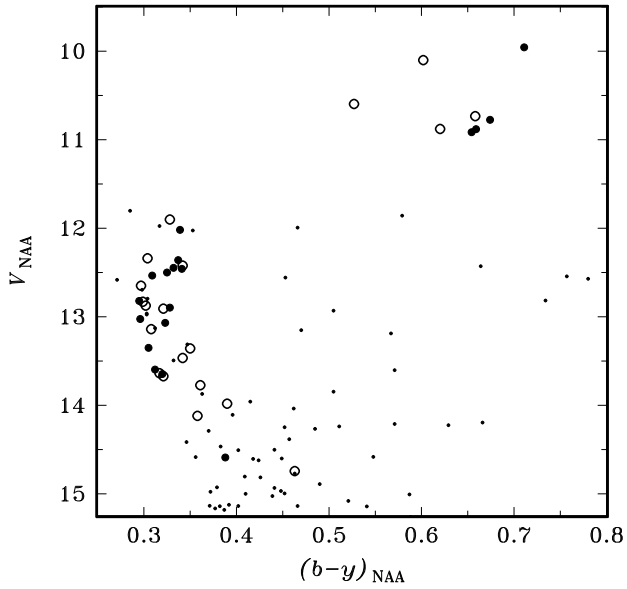


**Fig. 4.** *by* CMD for stars with CORAVEL observations. Small dots: Non-members; large dots: single members; open circles: binary members

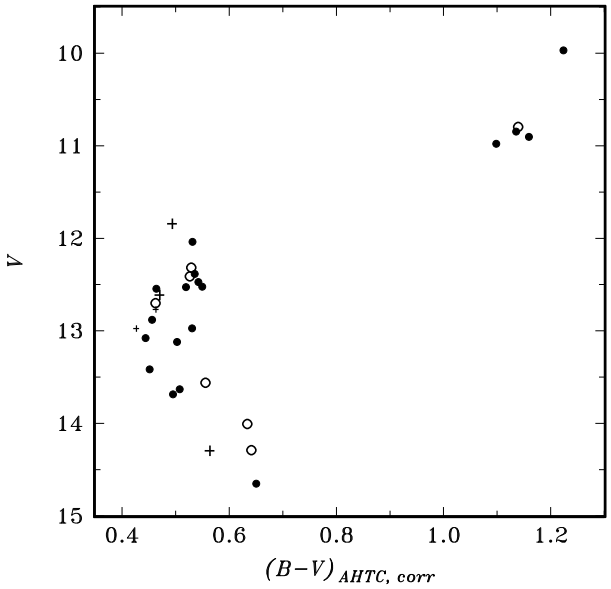


**Fig. 5.** CMD from the corrected AHTC *(B-V)* photometry (see Paper I). Filled circles are single member stars in the CCD field. Open circles are stars in the outer field satisfying the membership criteria. Plusses are broad-lined proper-motion members in the CCD field (small symbols) and outer field (large symbols)

statistics and mass estimate for NGC 3680, assuming they are binaries, but ignore them when fitting isochrones to the cluster sequence.

The $BV$ CMD of Fig. 5 shows the distribution of the 7 candidate outer-field cluster members, defined by the same criteria as in the inner field (obvious field stars not shown). While interlopers are more likely in the outer zone of the AHTC field, dynamical evolution is also expected to drive the low-mass stars into the outer regions of the cluster. As seen, some four plausible cluster stars (53, 3095, 4028, 4081) are added to the 35 or so in the inner field, with 3 probable interlopers (60, 4114, 4121) away from the cluster locus. As the areas of the outer and inner fields are roughly equal, this is consistent with the number of presumed foreground stars in the CCD field (note that all six lie above the cluster sequence).

For 8 stars in Table 1, no cross-correlation signal could be obtained with CORAVEL although their colours indicate that they should be observable with the K2 III mask of CORAVEL, probably due to rapid rotation in single stars or short-period binaries. Hence, for these stars, membership assignment in Table 1 has been made from proper motions alone. The five proper-motion members in this group are also shown in Fig. 5: The two inner-field stars 42 and 72 (K) and the two outer-field stars 1124 and 2110 fall near the cluster locus in the CMD and might have consistent radial velocities if observed with another instrument.

The outer-field candidate 78 (R) is in a location indicating a non-member or binary. We have tentatively included the outer-field radial-velocity members in our membership statistics, but not the stars without radial velocities; with the small number of stars, our conclusions on the cluster population and mass will not be affected materially.

Finally, we note that only 2 of the likely outer-field cluster members are in the NE and SW quadrants of the AHTC field, while 7 are in the NW-SE quadrants. Thus, the cluster may be somewhat elongated in a direction roughly along the galactic plane, as expected theoretically and recently seen for M67 by Fan et al. (1996).

### *3.2. Reddening, metal abundance and distance of NGC 3680*

Several determinations of the metal abundance and reddening of NGC 3680 exist (AHTC and references therein). The most direct and reliable values are from the *uvby-$H_\beta$* photometry of 32 F-type dwarfs in NGC 3680 by N88, who obtained [Fe/H] = 0.09±0.08 (s.d.) and $E_{(b-y)}$ = 0.034, corresponding to $E_{(B-V)}$ = 0.05 (consistent with the original $UBV$ result by Eggen 1969).

After the analysis above, only 9 of these 32 stars are both cluster members and single (excluding E4 and E35 which fall outside the cluster sequence, see above). Only three of these (E10, 37, and 43) have $\beta$ indices allowing direct determination of $E_{(b-y)}$. The mean reddening for these three stars is $E_{(b-y)}$ = 0.031±0.005 (s.d.), while the mean metallicity for all 9 single members is [Fe/H] = 0.11±0.05 (s.d.). Both values are entirely consistent with the means for all stars assumed to be members by N88, while the dispersion of the individual values is reduced as one would expect. We adopt in the following a mean reddening of $E_{(b-y)}$ = 0.034 or equivalently $E_{(B-V)}$ = 0.05 and note that the mean metallicity of [Fe/H] = 0.11±0.02 (s.d. of mean) is identical to that of the Hyades ([Fe/H] = 0.12, Cayrel et al. 1985). The apparently discrepant spectroscopic value [Fe/H] = -0.15 by Friel & Janes (1993) is easily explained, as three of their seven stars are in fact non-members and two are binaries with blue secondaries.

The average metallicity of the 8 F-type non-members observed by N88 and for which the $uvby\beta$ calibrations are valid is [Fe/H] = 0.15±0.15 (s.d.), and E16 has $E_{(b-y)}$ = 0.031. Thus, the field stars have compositions and reddenings very similar to NGC 3680 itself, further complicating the separation of cluster and field stars.

Numerous determinations of the distance of NGC 3680 exist (reviewed by AHTC), based on methods ranging from photometry of individual stars to CMD fits of theoretical isochrones. The results span a range in *(m-M)*$_0$ from at least 9.6 to 10.3. We have made a direct distance determination by fitting the lower main sequence of NGC 3680 to that of the Hyades, taking advantage of their identical metallicities and small and well-determined reddenings. Three obstacles are, however: *(i)* The poor quality of the $BV$ photometry of NGC 3680; *(ii)* only one $bona\ fide$ single cluster star on the lower main sequence (E70=I) appears in the CCD field, and *(iii)* at this mass, the isochrone already deviates somewhat from the ZAMS. We have tried to alleviate these difficulties by using *(i)* our new *by* CMD; *(ii)* an appropriate isochrone to fit the entire cluster locus and not rely on a single star, and *(iii)* the fitted isochrone to correct for the evolution of E70 away from the ZAMS.

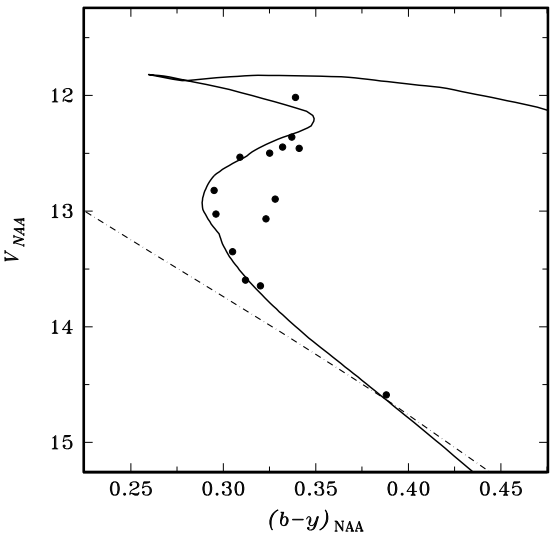


**Fig. 6.** The fit of the Hyades main sequence (dot-dashed line) to the single member stars of NGC 3680 (dots). The solid line is the S92 isochrone for the Hyades metallicity (see text)

The latest convergent-point analysis of the Hyades is by Schwan (1991), who gives the standard main sequence ($M_v$,*(B-V)*) for the resulting distance modulus of *(m-M)*$_0$ = 3.40, a value supported by the recent analysis of Hyades binaries by Torres et al. (1997). We have transformed this main-sequence relation to the Strömgren system via a plot of the *(B-V)* values listed by Schwan (1991) vs. the observed *(b-y)* indices for the same stars from Crawford & Perry (1966) and Olsen (1993). Fig. 6 shows the resulting fit of the Hyades main sequence to NGC 3680 as represented by the 1.45 Gyr isochrone by Schaller et al. (1992; S92) interpolated to the Hyades metal abundance (see Sect. 4.3), both curves being reddened by $E_{(b-y)}$ = 0.034.

The fit to the cluster, isochrone and Hyades relation in Fig. 6 is reasonably good, but the curves do not converge exactly at the lower end. There is also a slight inconsistency between the distance moduli needed for the Hyades main sequence (10.5) and the isochrone (10.25) to fit the cluster. However, while the *(B-V) - (b-y)* relation for the Hyades is well-established from an ample number and range of observed stars, the transformation used to transpose the isochrone to the *(b-y)* CMD is extrapolated and thus less reliable for *(b-y)* $>$ 0.40, just where the isochrone joins the unevolved main sequence. Thus, with a ZAMS slope of nearly 15 in the *(b-y)* CMD, plausible accumulated colour zero-point differences of only $\sim$ 0$^{\rm m}\!.$02 in the *(B-V)* and *(b-y)* observations and the colour transformations would suffice to reconcile these numbers.

We adopt the distance modulus derived here from the direct Hyades fit, *(m-M)*$_0$ = 10.5, with an estimated uncertainty of 0$^{\rm m}\!.$2. The resulting distance (1.26 kpc) is the largest found

for NGC 3680 so far. This is in principle understandable since the fit is now correctly made to the lower envelope of the broad distribution of cluster and field single stars and binaries in the main-sequence region. However, the discrepancy from the mean for the 9 single member stars from N88, $(m\text{-}M)_0 = 9.86 \pm 0.29$ (s.d.), is worrying since the latter is based on the standard *uvby*-$H_\beta$ calibrations for single stars and is thus unaffected by the errors discussed above. The *uvby* absolute-magnitude calibrations need to be reviewed, based on new HIPPARCOS parallaxes.

As a check we repeated the fit in the $BV$ CMD, using the corrected AHTC photometry (see Paper I), and found $(m\text{-}M)_0 = 10.3$. However, the fit of the theoretical isochrones to both the Hyades and NGC 3680 main sequences is poor, and the calibration and transformation problems encountered with both observed and computed broad-band colours (Paper I and Sect. 4) made it unattractive to pursue these fits any further. An attempt using the published Eggen (1969) *(B-V)* values directly also failed, because the Eggen *(B-V)* for E70 (I) is in error by more than $0\overset{\mathrm{m}}{.}20$, judging from a comparison with the AHTC photometry and the *by* CMD.

In conclusion, we adopt $(m\text{-}M)_0 = 10.5$ (1.26 kpc) as our current best estimate for the true distance modulus of NGC 3680, being based on the best-calibrated photometry and the smallest number of uncertain steps. With galactic coordinates of $(l,b) = (286\overset{\circ}{.}8, 16\overset{\circ}{.}9)$ and a distance of 1.26 kpc, NGC 3680 is then situated some 8.2 kpc from the galactic centre, close to the inner limit for old clusters (Friel 1995), and about 370 pc above the plane. All three components (*U,V,W*) of its space motion are below $\sim$2 km s$^{-1}$; i.e. it is moving along the solar circle trailing the Sun and essentially at rest with respect to us. The low contrast between cluster and field in both radial velocity and proper motions is a natural consequence.

### 3.3. Binary frequency in cluster and field stars

To the extent allowed by the precision, number, and time span of our CORAVEL observations, detection of spectroscopic binaries in NGC 3680 should be reasonably complete for periods less than $\sim$1000 days and velocity amplitudes larger than a few km s$^{-1}$. Since the binary population as such is not our primary interest here, field stars have not been followed systematically after their non-membership had become clear, so binary detection is less complete in the field. The actual results are as follows:

Amongst the 44 cluster stars fulfilling both our radial-velocity and proper-motion membership criteria, 25 binary systems have been detected, leaving 19 single stars, or a binary frequency of 57% in the period range mentioned. This is much higher than found for the nearby solar-type dwarfs by Duquennoy & Mayor (1991). This result should not be extrapolated to all periods using their period distribution, as there are strong reasons to expect an overabundance of closely bound binaries among the surviving stars in NGC 3680, which we show below to be in an advanced stage of dynamical evolution. With three definite spectroscopic binaries (E11, 20, and 27) amongst the 9 confirmed red-giant members and one obviously composite, if currently non-variable system (E34), the frequency of red-giant binaries (44%) appears marginally lower than on the main sequence. This is expected, since the shortest-period binaries will experience Roche-lobe overflow when leaving the main sequence and not evolve to the RGB.

Of the 65 field stars with radial-velocity data, 26 are classified as binaries while 36 appear single so far, a minimum binary frequency of 45%. Given their different observational histories, no significant difference between field and cluster samples can be claimed.

### 3.4. Spatial distribution of single and binary cluster stars

The virtual absence of lower main-sequence stars in NGC 3680 suggests that it is in an advanced stage of dynamical evolution, being possibly relaxed and having experienced mass segregation. To this end we have studied the cumulative distribution of different groups of stars as a function of their angular distance from the cluster centre. Defined as the mean of the coordinates of the cluster stars identified above (both single and binary members), the position of the cluster centre is:

$(\alpha_c, \delta_c)_{J2000} = (11^h25^m34\overset{s}{.}4, -43^\circ13'36\overset{''}{.}2)$

This position is close to the central bright giant E34 and the concentration of stars which also by visual inspection appears to mark the cluster centre.

Cumulative radial distributions of three groups of stars are plotted together in Fig. 7: Field stars, single cluster members, and cluster binaries. The expected $R^2$ form of the field star distribution is shown by a parabolic fit; the observed curve suggests that one or two stars near the centre and now classified as field stars could turn out to be (long-period) cluster binaries if observed long enough.

Within the limitations of the small number of stars, the two other curves show that the cluster binaries are more centrally concentrated than the single stars, as expected if mass segregation has occurred. The 1-$\sigma$ cluster radii derived for all members, single members alone, and binaries alone are $4.7'$, $6.0'$, and $3.5'$ respectively, in good agreement with the 1-$\sigma$ mean radius found by K95, $3.6 \pm 0.1'$. This result is derived only from stars in the $20'$ AHTC field; however, K95 covered a field of nearly one degree without detecting any halo of faint stars near the tidal radius of NGC 3680, estimated to be 4.2 pc or $14'$.

### 3.5. Rotational velocities of cluster and field stars

In Paper I, we determined rotational velocities for all programme stars from the CORAVEL cross-correlation profiles, using the calibrations of Benz & Mayor (1981, 1984). The distribution of these rotations is shown in Fig. 8, separately for cluster and field stars. In order for the samples to be as comparable as possible, only single stars with $0.4 < (B\text{-}V) < 0.7$ have been included. Hence, bias from slowly-rotating cluster giants and red field stars and from tidally synchronised binaries has been removed.

The two distributions are notably different, the field-star distribution peaking at slow rotations and the cluster stars showing

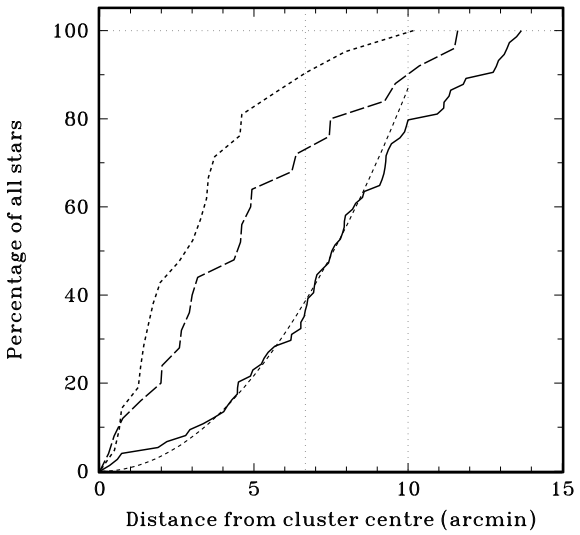


**Fig. 7.** Cumulative radial distributions of the binary (short-dashed) and single (long-dashed) members of NGC 3680, and of the field stars (solid) with an $R^2$ fit for comparison. The vertical dotted lines indicate the radii of circles inscribed in the square CCD and AHTC fields, respectively

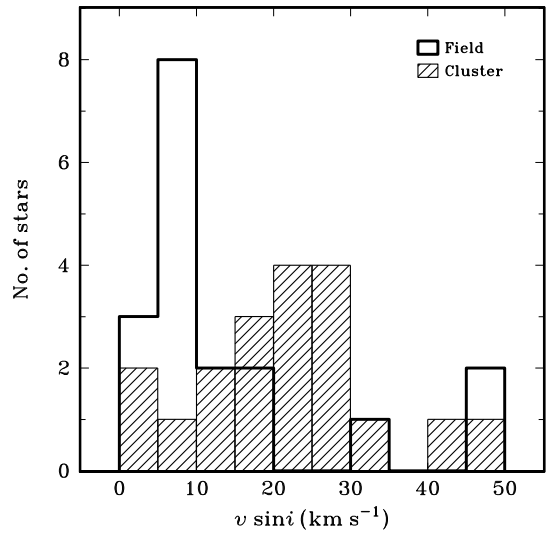


**Fig. 8.** Distribution of observed $v$ sin $i$ values of cluster and field stars with $0.4 <$ *(B-V)* $< 0.7$

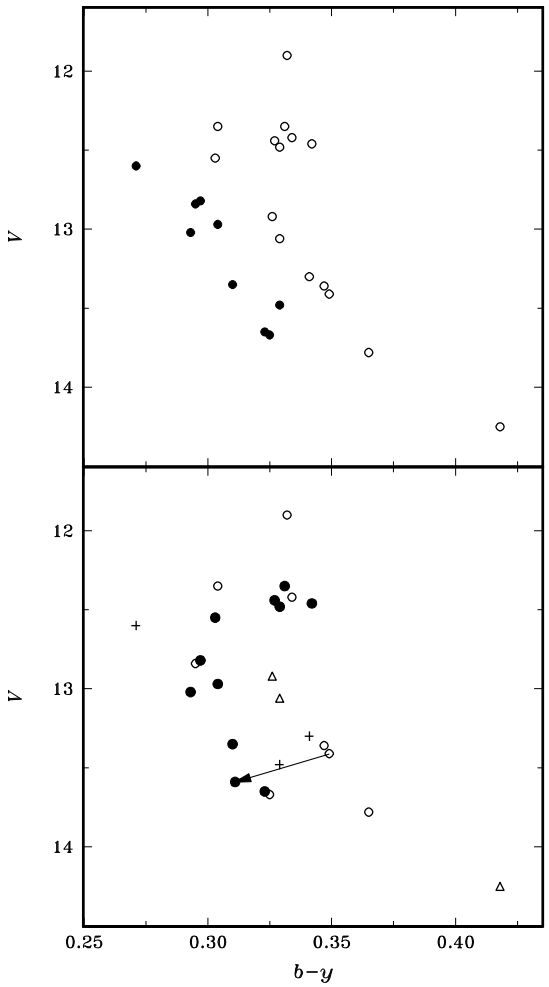


**Fig. 9.** Upper panel: Upper main sequence of NGC 3680 from N88 (Fig. 12), with stars assigned to red and blue branches as done there. Lower panel: Same stars identified as single members (dots), binary members (circles), field stars (plusses), and likely foreground stars (triangles). The arrow shows the effect of correcting the photometry of E30 for its close visual companion

a broad maximum at moderately fast rotations. This is understandable if the cluster stars are on average more evolved than the field, starting out as fast-rotating A-type stars (Slettebak 1970). *uvby-*$H_\beta$ photometry for both cluster and field samples would, in principle, allow to test this hypothesis.

### *3.6. CMD morphology and the "bimodal turnoff" of NGC 3680 revisited*

Comparison of Figs. 1, 4 and 6 quickly reveals the cause of the previous disagreements on the interpretation of the CMD of NGC 3680: The field star contribution is unusually strong, especially near the main sequence. In particular, almost none of the faint stars in the lower main-sequence region actually belong to the cluster as pointed out on statistical grounds by AHTC and K95, but confirmed here on a star-by-star basis. Moreover, the high binary frequency among the surviving upper-main-sequence stars creates the impression of a second sequence in the CMD, roughly parallel to the actual cluster main sequence.

The definition of a cluster sequence for comparison with theoretical isochrones is much improved by the new data, both in the main-sequence and giant regions (see Figs. 4 - 6). The characteristic turnoff curvature discussed by ATTS and AHTC, using preliminary results from the present study, is clearly and unambiguously defined. All four discrepant giants are established binaries; the remainder form a tight clump and giant branch while the previous "subgiant branch" consisted only of field stars.

A much-discussed feature of NGC 3680 was its "bimodal turnoff" (Twarog 1983; N88; ATTS). Attempts to interpret this as an effect of stellar evolution were inconclusive. As shown by Figs. 4 and 6, the bimodality disappears once binaries and nonmembers are removed from the CMD, as found also for the prototype "bimodal" cluster NGC 752 by Daniel et al. (1994).

While further search for an astrophysical explanation of the "bimodal turnoff" would seem unnecessary, it is instructive to see how simple effects conspired to produce the remarkably clean bifurcation seen in the careful study of N88. Fig. 9 shows the turnoff of NGC 3680 in the N88 $uvby$ CMD, using the sample of Figs. 11 and 13 of N88 and assigning the stars to the "blue" and "red" sequences following N88. A crucial feature is the group of stars composed by E16, E22, and E30: E16 is in reality a binary and non-member, E22 a double-lined binary, and E30 a close visual double. The CCD data for E30A alone place it on the blue sequence in the CMD. Assuming that E4 and 35 are field stars or binaries (see Sect. 3.1.2) completes the picture. Note also that the two separate sequences, but not the real cluster, can be fit by the standard isochrones then believed to be valid for NGC 3680.

## 4. Analysis

Having defined a precise observed cluster sequence in NGC 3680, we turn in the following to a detailed comparison with stellar evolution models. Like the observational phase of the study, this was not without surprises.

### *4.1. Review of theoretical evolution models and colour transformations*

The major modern, published series of stellar models for metallicities near that of NGC 3680 fall in two classes according to the type of convection description employed: "Standard" models using the classical Schwarzschild criterion for the transition between radiative and convective regions, and "overshooting" models assuming convection to penetrate some distance into the adjacent radiative region, typically by some fraction $\alpha$ of a pressure scale height $H_p$. The formalism may be applied to convective envelopes as well as cores, but since processes in the core are responsible for the main features of stellar evolution, "overshooting" in the following will refer to convective cores (i.e., for masses above $\sim$1.2 $M_\odot$).

The following models have been considered:

*Standard models.* Two sets of model computations have been considered: First, the solar-metallicity models of VandenBerg (1985), based on the 1977 Los Alamos opacity library (Huebner et al. 1977), to which we have applied the temperature and colour corrections recommended in the later discussions of boundary conditions and colour scales by VandenBerg & Poll (1989) and Pedersen et al. (1990). Second, the models by Castellani et al. (1992), using the same opacity data and also computed for solar metallicity.

*Overshooting models.* Three sets of overshooting models exist in the literature, all using the latest OPAL opacities (Iglesias et al. 1992; Rogers & Iglesias 1992) and an overshooting parameter $\alpha = 0.20$. Limiting ourselves for the moment to solar-composition models ($Z$ = 0.02, $X$ = 0.70), the three series are those by Claret (1995), the Geneva group (S92; Schaerer et al. 1993), and the Padova group (Bertelli et al. 1993, 1994). In addition, a new (still preliminary) set of models by Dowler & VandenBerg (1996; DV96) was kindly made available to us before publication; these also use OPAL opacities, incorporate convective overshooting in the Roxburgh (1978, 1992) formulation, and are computed for the metal abundances of both the Sun and the Hyades (= that of NGC 3680).

First, we have investigated the interagreement of the various models by comparing what should be the same (solar-composition, 2-Gyr) isochrone from all six series. All isochrones provide effective temperatures and luminosities, absolute visual magnitudes, and broad-band *(B-V)* colours.

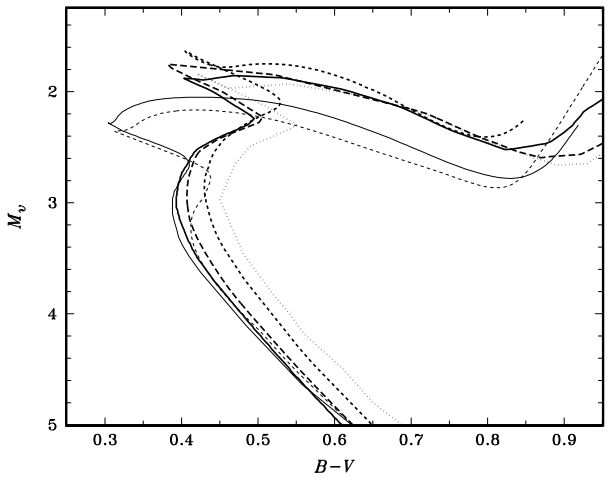


**Fig. 10.** Solar-metallicity 2-Gyr isochrones in the *(B-V)*, $M_v$ diagram. Thin lines: Standard models: VandenBerg (1985; full); Castellani et al. (1992; dashed). Thick lines: Overshooting models: S92 (full); Claret (1995; long-dashed); DV96 (short-dashed); Bertelli et al. (1993; dots)

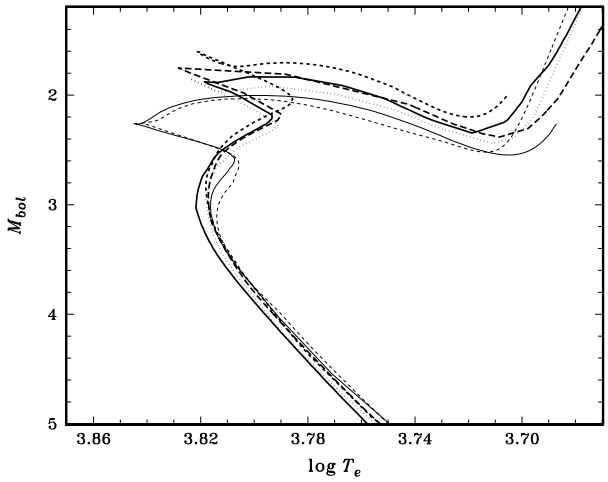


**Fig. 11.** Solar-metallicity 2-Gyr isochrones in the theoretical HR diagram. Models are identified by line type as in Fig. 10

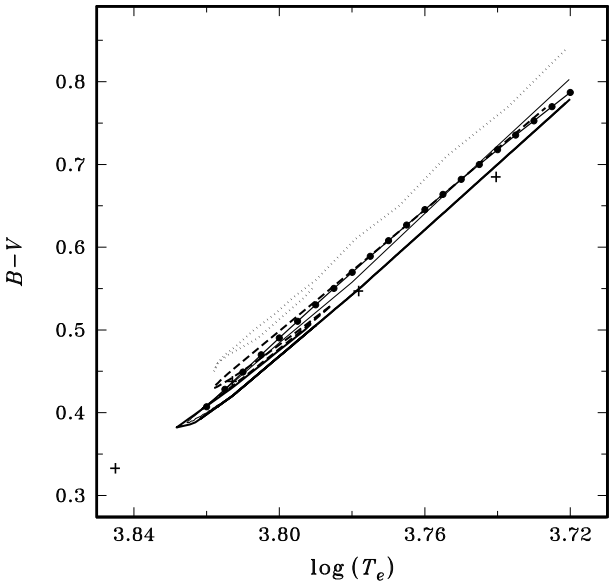


**Fig. 12.** $T_{\rm eff}$ - *(B-V)* colour transformations for the models of Figs. 10 and 11 (same line types), and theoretical relations from Saxner & Hammarbäck (1985; dots) and VandenBerg & Bell (1985; plusses)

Fig. 10 displays all six isochrones, as published, in the *(B-V)*, $M_v$ diagram. Two main features stand out: *(i):* The clear qualitative difference in the turnoff shapes of standard and overshooting models, and *(ii):* The wide range in main-sequence colours at given luminosity. These discrepancies were also discussed by ATTS and AHTC, who attempted to correct for the differences in opacity data, convection prescriptions, etc., by applying colour and luminosity shifts to the published models (see also Anthony-Twarog et al. 1993). It is not obvious, however, that the differences between various models are adequately described by such shifts, usually derived from the standard requirement that models should fit the present Sun. Since the Sun has no convective core, however, different treatments of convection in the cores of more massive stars, such as those in NGC 3680, cannot be accounted for by this procedure.

In order to identify the origin of the observed discrepancies, we plot in Fig. 11 the same models in the theoretical HR diagram. Evidently, all models now agree well on the lower main sequence, and standard and overshooting models agree very well internally at the turnoff, while the difference between the two groups persists. Thus, the models are in fact physically very similar, and the discrepancies seen in Fig. 10 arise primarily in the transformations from chemical composition, effective temperature, and gravity to observable *(B-V)* indices.

Accordingly, we show in Fig. 12 the colour transformations used in the different models. Clearly, these relations disagree by several hundredths of a magnitude in *(B-V)*, another manifestation of the standing controversy over the colour of the Sun (see, e.g. VandenBerg & Poll 1989); differences in the scales of bolometric corrections in the different models are unimportant. Given the difficulty of computing realistic and precise broad-band colours from synthetic spectra even today (see, e.g. Bell et al. 1994), and the difficulties encountered in Paper I with the observed $BV$ photometry in NGC 3680, we decided to disregard *(B-V)* colours in most of the following discussion.

As expected, the situation is substantially better when using intermediate-band Strömgren *(b-y)* colours instead. First, our new $by$ photometry is very well-calibrated in the main-sequence and turnoff region (but not for the red giants). Second, *(b-y)* colour transformations for F dwarfs, including explicit dependence on metallicity, have been published by, e.g. VandenBerg & Bell (1985), Saxner & Hammarbäck (1987), and Edvardsson et al. (1993). Again, there are somewhat disconcerting differences between these sources, and the cautionary comments of Bell et al. (1994) apply to the $uvby$ colours as well. However, for the remainder of this discussion we adopt the colour transformations from the most recent paper (Edvardsson et al. 1993), noting the good fit to the solar flux spectrum achieved there. Given the good consistency of the bolometric corrections of the different isochrones, we have used the computed $M_v$ values as published.

The models considered so far are for the solar metal abundance, while the metallicity of NGC 3680, similar to that of the Hyades, is about 30% higher. Two effects must be taken into account: Higher-metallicity models *(i):* are cooler and fainter, and *(ii):* have redder colours for the same effective temperature. DV96 have computed models for the Hyades composition, including broad-band colour transformations appropriate for this metallicity and thus directly applicable to the observations of NGC 3680. As the other main-sequence models are very similar in the theoretical HR diagram, it suffices to interpolate in one set to produce an approximation to Hyades-metallicity isochrones. We have done this by linear interpolation in the log$T_{\rm eff}$ and $M_v$ of the Geneva models for $Z$ = 0.02 and $Z$ = 0.04 (S92; Schaerer et al. 1993), subsequently deriving $(b\text{-}y)_0$ colours from $T_{\rm eff}$ and the Edvardsson et al. (1993) calibration for [Fe/H] = +0.1 ($Z$ = 0.026).

As observational errors still allow the possibility that the metallicity of NGC 3680 could be solar, we pursue the comparisons in the following under both assumptions.

### *4.2. Isochrone fits to the CMD of NGC 3680*

NGC 3680 has been repeatedly discussed as a possible discriminator between models with and without overshooting: Mazzei & Pigatto (1988) fit solar-metallicity models to Eggen's (1969) $BV$ CMD of NGC 3680, using the isochrone shape as the main fitting criterion. ATTS and AHTC also found overshooting models to give the best fit to their data. Castellani et al. (1992), on the other hand, fit standard models to the ATTS $by$ photometry of NGC 3680 and on this basis categorically dismissed the claims for significant overshooting by Mazzei & Pigatto, ATTS, and Andersen et al. (1990). Yet, Carraro et al. (1993) again found the same data to require overshooting models. Thus, a closer re-examination appears to be in order.

Apart from inadequacies in the old photometry used by Mazzei & Pigatto (see Paper I), three aspects of their study

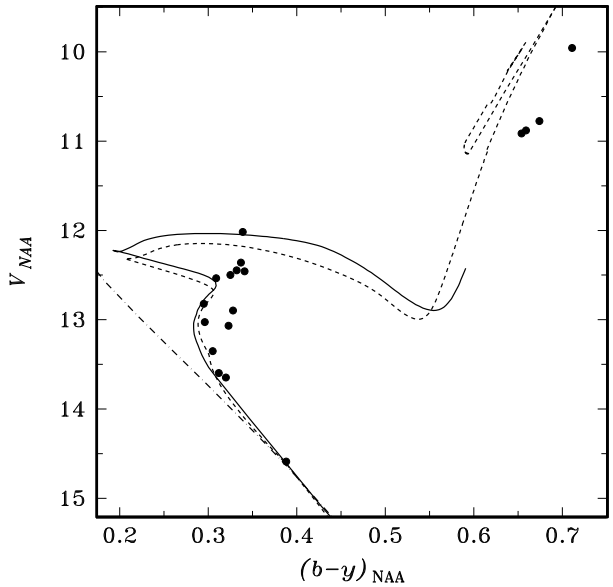


**Fig. 13.** Isochrone fit to the single members of NGC 3680 for the solar-metallicity standard models of VandenBerg (1985; full) and Castellani et al. (1992; dashed), both for an age of 1.5 Gyr and *(m-M)*$_0$ = 10.25

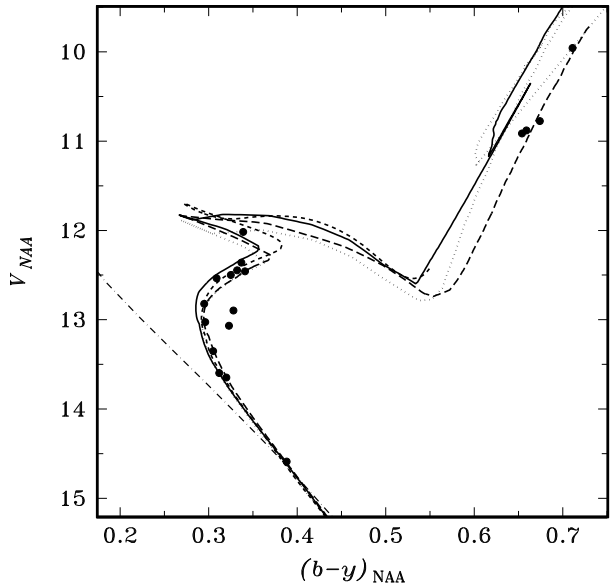


**Fig. 14.** As Fig. 13, but for the solar-metallicity overshooting models of S92 (1.6 Gyr, *(m-M)*$_0$ = 10.17; full), Claret (1995, 1.6 Gyr, *(m-M)*$_0$ = 10.28; long-dashed), DV96 (1.6 Gyr, *(m-M)*$_0$ = 10.25; short-dashed), and Bertelli et al. (1993, 1.6 Gyr, *(m-M)*$_0$ = 10.25; dots)

as well as those of Castellani et al. (1992) and Carraro et al. (1993) deserve comment:

First, all three studies include the reddening as a free parameter although it is in fact observationally well-determined (cf. Sect. 3.2). Moreover, the data are sometimes corrected in non-obvious ways (compare, e.g. Fig. 10 of Castellani et al. and Fig. 13 of Carraro et al. with the original *(b-y)* data by ATTS). All three adopt reddenings that are considerably larger than the true value and thus fit the CMD with models that are bluer, hence younger and more massive than the actual cluster stars. In effect, this procedure ignores the first-order age information (turnoff colour) in favour of a second-order effect (turnoff shape); as shown by Demarque et al. (1994), one can obtain almost any desired age by this method.

Second, the raw CMD (Fig. 1) leaves the choice of stars to be used in the fit wide open when no information is available on cluster membership and duplicity. The warning by Andersen et al. (1990) that the numerous field stars and binaries must be avoided in a proper fit was heeded by Carraro et al. (1993), while the summary dismissal of overshooting models by Castellani et al. (1992) was in fact based on a fit including field stars and binaries.

A third weak point in these studies is the use of solar-metallicity models to fit the more metal-rich NGC 3680. However, apart from leading to a slightly higher age estimate, this is in fact a minor problem compared to the two previous items. Still, a first condition for a truly *critical* test, i.e. one which is capable of excluding at least some of the possible contenders, is that *all* available observational constraints are satisfied, minimizing the number of adjustable parameters.

Our own isochrone fits in NGC 3680 are based on the following specific assumptions: *(i):* Model $M_v$ values are used as published; *(b-y)*$_0$ colours are computed from the model $T_{\rm eff}$ values and the transformations of Edvardsson et al. (1993) for the metallicity of each isochrone; *(ii):* isochrones are shifted in colour corresponding to a reddening of $E_{(b-y)} = 0.034$ and in apparent magnitude by $A_v = 4.3 \times E_{(b-y)}$ (Crawford & Mandwewala 1976). The true distance modulus is then adjusted to fit the isochrone to the cluster main sequence as represented by star E70 (I) and the Hyades ZAMS, similarly reddened and shifted as detailed in Sect. 3.2. Note that both theoretical and observed *(b-y)* colours are only properly calibrated in the F-dwarf domain, so the fit is less reliable for *(b-y)* $> 0.40$, and no meaningful fit to the cluster giants is possible.

For clarity, our isochrone fits to NGC 3680 are shown in three separate diagrams: Fig. 13 shows the two best-fitting solar-metallicity standard models, Fig. 14 the four best-fitting solar-metallicity overshooting models, and Fig. 15 the best-fitting Hyades-metallicity DV96 (computed) and Geneva isochrones (interpolated). It is seen, first, that all models fit the unevolved main sequence and lower turnoff very well and for remarkably consistent ages and distance moduli, underscoring the importance of using consistent colour transformations. Second, standard models cannot account for the group of upper turnoff stars at *(b-y)* $\approx 0.35$ and therefore are not acceptable for stars in this age and/or mass range. Third, all three published overshooting model series (Claret, Geneva, Padova) yield acceptable and essentially equivalent fits to the turnoff. The fact that they extend slightly beyond the observed turnoff may suggest a further small reduction in overshooting parameter, perhaps to near 0.1 $H_p$ as preferred for the Sun from helioseismological data (Christensen-Dalsgaard et al. 1995), an interesting convergence of techniques.The DV96 isochrone extends even further beyond

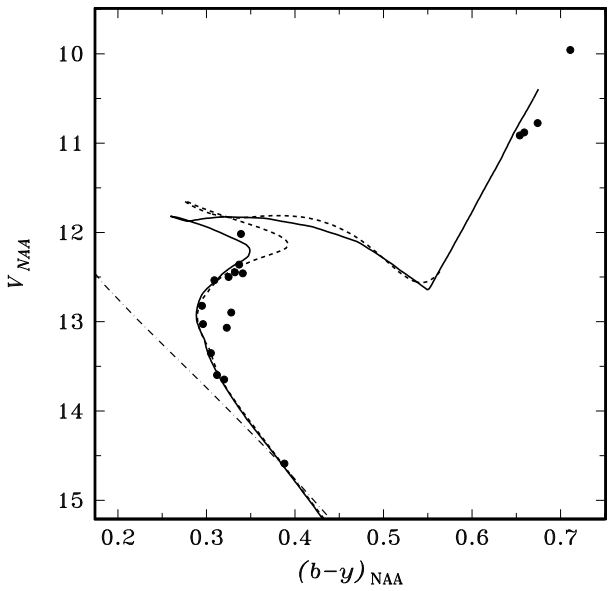


**Fig. 15.** As Fig. 13, but for the Hyades-metallicity overshooting models of S92 (1.45 Gyr, *(m-M)*$_0$ = 10.25; full) and DV96 (1.4 Gyr, *(m-M)*$_0$ = 10.3; short-dashed)

the observed turnoff; the effective amount of overshooting may be somewhat overestimated by the Roxburgh formalism in these models. Finally, standard and overshooting models yield the same age for the same composition, and ages from solar- and Hyades-metallicity models differ by only ∼10%.

We consider the result that standard models cannot account for the turnoff shape in NGC 3680 to be a firm conclusion. As the metallicity of NGC 3680 is close to that of the Hyades, our best fits appear to be with the corresponding interpolated 1.45-Gyr Geneva isochrone (S92) and the 1.4-Gyr isochrone of DV96. We return in Sect. 5.2 to a discussion of the accuracy and consistency of the distance and age estimates for NGC 3680.

### *4.3. Masses of the cluster stars*

With best-fit isochrones now identified, we proceed to derive masses for the individual cluster stars. In binaries, masses are estimated so that the components fit the isochrone and yield the observed combined luminosity. Masses derived from the two selected isochrones differ by only 7%, implying masses at the redward tip of the turnoff of 1.8 $M_\odot$ for S92, 1.95 $M_\odot$ for DV96.

Interestingly, however, we can in fact discriminate between these two possibilities: The evolved F-type component of the eclipsing binary TZ For (Andersen et al. 1991) has a mass of just 1.95 $M_\odot$ and a *(b-y)* colour equal to the red tip of the turnoff of NGC 3680. Thus, if the DV96 isochrones accurately represent the cluster stars and TZ For were moved to the same distance, TZ For A would fit the tip of the turnoff in the cluster CMD (and the K-type giant TZ For B the giant clump). In fact, TZ For A is about half a magnitude brighter and thus more massive and younger than the turnoff stars in NGC 3680. The S92 isochrone, however, predicts just about the right luminosity difference between its 1.8 $M_\odot$ turnoff stars and TZ For A, so we shall use these models in the following. The bluest point of the isochrone occurs at 1.6 $M_\odot$.

From 44 cluster stars containing 69 individual components, the present total mass of NGC 3680 (within the 20′ AHTC field) is 96.5 $M_\odot$, somewhat less than estimated by K95. The average mass of a cluster star is 1.5 $M_\odot$, but the mean masses are clearly different for single stars (1.7 $M_\odot$), binary members (1.3 $M_\odot$), and secondaries in binary systems (1.1 $M_\odot$; all ± ∼0.05 $M_\odot$). No heavy remnants (white dwarfs, neutron stars) are included in these figures. From the cumulative radial mass distribution in NGC 3680 we find a half-mass radius of 3.3′ or 1.2 pc, in the lower range of typical cluster sizes (Friel 1995), consistent with its modest mass and advanced evolution.

## 5. Discussion

Considered to be a relatively well-studied cluster, NGC 3680 is included in the small group of "reference clusters" used to calibrate various observational parameters from which general properties, notably ages, are derived for clusters with less complete data (see, e.g. Friel & Janes 1993; Janes & Phelps 1994; Carraro & Chiosi 1994; Friel 1995). Our more definitive study of the cluster does, however, show it to be atypical in a number of respects of importance for several standard analysis techniques. We discuss these aspects in the following.

### *5.1. Luminosity and mass function of NGC 3680*

As shown by AHTC and K95 and mentioned above, the luminosity function of NGC 3680 is clearly abnormal, with a striking lack of cluster stars fainter than $M_v \approx 4$. Our detailed identification of single and binary cluster members and field stars reinforces this conclusion: Even the modest number of cluster stars below $V$ = 14 estimated by K95 was inflated by proper-motion errors, as discussed by K95 themselves. Evidently, NGC 3680 is in an advanced stage of dynamical evolution, its low-mass stars having been lost from the inner parts of the cluster and the binary stars being concentrated towards the centre. Having estimated masses for every cluster star identified in the observed field, we are in a position to assess the dynamical state of the cluster in more quantitative terms. The remaining few stars for which membership and/or duplicity are still doubtful are unimportant for our conclusions.

Fig. 16 shows the present-day mass function for NGC 3680, separately for single stars and all (single or binary member) stars. Again, the peak in the turnoff and giant region and the high binary frequency stand out: stars with masses $\lesssim 1.4 M_\odot$ essentially only survive in binary systems. As all normal initial mass functions (IMFs) show a distinct *rise* towards smaller masses, the initial cluster population must have been severely eroded.

We have estimated the original cluster population by fitting the IMFs by Salpeter (1955), Miller & Scalo (1979), and Kroupa et al. (1993) to NGC 3680, normalizing the total number of stars

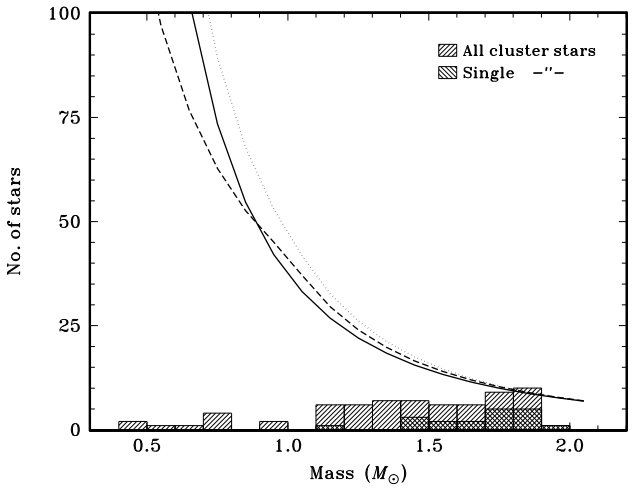


**Fig. 16.** Observed present-day mass function of NGC 3680. Lines show the IMFs by Salpeter (1955; solid), Miller & Scalo (1979; dashed) and Kroupa et al. (1993; dots), normalised to the highest mass bin

in the range 0.1-60 $M_\odot$ so as to match the number now observed in the 1.8-1.9 $M_\odot$ bin. While stars may have been lost also in this mass range, this procedure should give a conservative estimate of the total mass lost from the cluster.

Under these assumptions, we find the following results for the initial number of stars and total mass of NGC 3680, including all binary components: ($N_{ini}$, $M_{ini}$) = (2000, 1200$M_\odot$), (3600, 1600$M_\odot$), and (11000, 2200$M_\odot$) for the Miller-Scalo, Kroupa et al., and Salpeter IMFs, respectively. Adopting the Miller-Scalo form as the least extreme (and we note that Padoan et al. 1996 find both theoretical and observational support for an IMF of this form), we still find that NGC 3680 now contains fewer than ∼3% of its original stars and less than ∼10% of its initial mass - a small tip of the proverbial iceberg.

Considering that this aspect is usually ignored entirely, the actual degree of depletion is dramatic. It is, in fact, already visible in the simulations of cluster CMDs, typically assuming a Salpeter IMF, by e.g. Mazzei & Pigatto (1988) and Carraro et al. (1993). Uncorrected cluster luminosity functions would appear to be of limited value under such circumstances. Our result for NGC 3680 is, nonetheless, qualitatively similar to what is found in a few other, less extreme clusters (Friel 1995 and references therein), and quite in line with the predictions of numerical N-body simulations for the dynamical evolution of open clusters like NGC 3680, assuming realistic IMFs and binary frequencies (Terlevich 1987; de la Fuente Marcos 1995, 1996ab; Aarseth 1996; Eggleton 1996).

Mass loss from a cluster during its evolution is due to two different processes: Evolution of high-mass stars and evaporation of low-mass stars. With a present turnoff mass just below 2 $M_\odot$, the more massive initial members of NGC 3680 have now completed their evolution to the white dwarf stage or, for the most massive stars, presumably undergone supernova explosions and ejected their neutron star remnants from the cluster. All three IMFs considered above predict that NGC 3680 initially contained of the order of 100 stars in the mass range 2-60 $M_\odot$, with a total mass of ∼400$M_\odot$ or ∼30% of the initial total mass. Thus, stellar evolution alone accounts for the loss of the upper ∼30% of the original cluster mass, but in principle as much as 70 $M_\odot$ of this might still be present in the form of heavy remnants, presumably white dwarfs. A deep UV survey of the centre of the cluster might be able to detect these white dwarfs, if still present, below $V \approx 22$.

Low-mass stars are lost from the central regions of the cluster due to mass segregation and galactic tidal effects, especially in poor clusters (de la Fuente Marcos 1995). The former results in the low-mass stars forming a halo 1-2 tidal radii from the cluster centre (Terlevich 1987). K95 estimate the tidal radius of NGC 3680 to be about 4.2 pc or 14″ on the sky. The field surveyed by them extended to ∼4 tidal radii, but no halo of faint proper-motion members was found. Given the uncertainty in the actual total mass and extent of the cluster, the tidal radius is poorly determined, and we note that for the somewhat more massive cluster NGC 2420, Leonard (1988) derived a tidal radius of more than half a degree on the sky. A determined search for faint cluster members outside the AHTC and K95 fields would therefore still be of interest, as recently done for the old cluster M67 by Fan et al. (1996). Our isochrone fit for NGC 3680 itself defines the locus in the CMD where outlying lower-main-sequence stars should be found.

If not eventually found in an outer halo around NGC 3680, the original lower-main-sequence stars have presumably been stripped from the cluster altogether, due to a passage of NGC 3680 close to a giant molecular cloud or similar massive object. The calculations of Terlevich (1987) indicate that a single such (rare) passage is sufficient to disrupt the cluster in rather short order. The precise conditions of such an encounter appear to be crucial for the outcome, but the theory seems to be developing to the point where a direct, detailed numerical simulation of the dynamical history of NGC 3680 appears possible and likely to be informative.

### *5.2. NGC 3680 and tests of stellar evolution models*

Our conclusion that standard models do not fit NGC 3680 appears firm, since cluster stars exist beyond the predicted turnoff of these models. At first sight, the very tight cluster sequence defined by our new *by* photometry and clean selection of member stars (Fig. 13-15) would also appear to allow further tuning of the overshooting parameter.

Reality is, however, not as clear-cut. First, the small number stars in NGC 3680 prevents a secure definition of the tip of the turnoff (although the apparent accumulation of stars there is intriguing). Second, the concept of describing the complicated hydrodynamics of real convective motions in stellar cores by a single parameter is no doubt a gross oversimplification. Fortunately, more realistic convection schemes are under development (Zahn 1991; Canuto & Mazzitelli 1992; Nordlund & Stein 1996), and further precise studies of clusters of different ages and turnoff masses should help to check their validity.

Third, as discussed in Sect. 4.1, the colour transformations and bolometric corrections used when comparing models and real stars are by no means in a definitive state, even for F dwarfs of near-solar metallicity, although the improved consistency of fits using a single colour transformation is encouraging.

Finally, as neither observed nor computed $uvby$ colours are properly calibrated for the red giants, we have not made isochrone fits to these stars. However, with a turnoff mass in the range of upper limits for the He flash in overshooting models (Maeder & Meynet 1989), NGC 3680 might yield further interesting results from such comparisons.

### *5.3. The age of NGC 3680*

The use of NGC 3680 as a standard cluster for calibration purposes makes its true age of more than passing interest. Indeed, a main motivation for initiating this study was the large discrepancy then existing between ages for F-type dwarfs as derived from standard and some overshooting models: Previous age estimates for NGC 3680 covered a range from 1.0 Gyr (Mazzei & Pigatto 1988) to 4.5 Gyr (AHTC), a difference of no small importance for studies of the evolution of the galactic disk.

Apart from a specific model problem which led to the single high value and has been resolved in the meantime (S92; Bertelli et al. 1992), causes of this scatter include *(i):* Overcorrection for reddening, leading to overestimated turnoff temperatures and low ages; *(ii):* colour transformations giving too blue or too red colours, i.e. over- and underestimated ages, respectively; *(iii):* use of models of lower (solar) metallicity than that of NGC 3680, giving too blue turnoff colours and too high age; and *(iv):* an assumed distance that is either too low, leading to underestimated luminosities and overestimated ages, or the reverse.

In contrast, our own isochrone fits for the precise reddening and metallicity determined for NGC 3680 by N88 lead to remarkably consistent results, with all standard and overshooting solar-metallicity models yielding very nearly the same distance moduli and ages (see Sect. 4.2). We note, however, that colour transformations are still not very secure for *(b-y)* $\gtrsim$ 0.40, and further improvement remains desirable. For the moment, we estimate the resulting age for NGC 3680 to be uncertain by perhaps 20%, excluding systematic errors in the models themselves.

## 6. Conclusions

The photometry, radial velocities, and proper motions discussed in this paper place NGC 3680 in a very small group of open clusters with data at this level of detail and completeness. The recent study by Daniel et al. (1994) of the similar, but richer cluster NGC 752 is analogous to ours, but also differs in certain respects. Our more complete radial-velocity coverage and rigorous membership criteria are both more effective and more necessary in the sparse NGC 3680. Also, the zero-point uncertainties in both observed and model broad-band colours (Daniel et al. 1994; Paper I) reinforce our preference for intermediate-band photometry in precise work (cf. our Figs. 10-15).

Our study has transformed the traditional view of NGC 3680: Far from being an uncomplicated cluster that can be simply modelled by an average isochrone populated by stars following a Salpeter IMF plus some photometric scatter, NGC 3680 is revealed as the last remnants of a cluster in an advanced state of dissolution, almost lost in a field of foreground stars of very similar characteristics. Thus, as perhaps the most significant result of this study, NGC 3680 should serve as a warning of the fragility of conclusions drawn from fits to raw cluster CMDs.

Our main results on NGC 3680 itself can be summarised as follows:

1. Combining individual radial-velocity and proper-motion membership probabilities, we find 76 field stars out of the total of 120 observed.
2. Among the 44 cluster stars, 25 or 57% are found to be binaries.
3. From the single member stars, NGC 3680 is found to have mean values of $E_{(b-y)}$ = 0.034, [Fe/H] = +0.11. A direct fit to the Hyades main sequence yields a true distance modulus of $(m\text{-}M)_0$ = 10.5.
4. The single-member cluster sequence in the CMD shows that standard models do not match the true shape of the turnoff; overshooting models perform much better, but further improvement is possible.
5. Using a consistent colour transformation to Strömgren *(b-y)* colours produces excellent fits to the observed CMD for consistent ages and distances for all models. The best-fitting overshooting isochrone for the observed metallicity yields an age of 1.45 Gyr for NGC 3680, with an estimated overall uncertainty of $\sim$20%.
6. The best-fitting isochrone gives a mass of 1.8 $M_\odot$ for stars at the tip of the turnoff of NGC 3680, verified with eclipsing binary data. Assigning masses star by star, we find the 69 cluster stars to have a present total mass of $\sim$100 $M_\odot$; stars below 1.4 $M_\odot$ are now only found in binaries. The half-mass radius of NGC 3680 is 3.3′ or 1.2 pc; and binary cluster members are more centrally concentrated than the single stars.
7. Fitting a selection of IMFs to the possibly undepleted high-mass end of the observed mass function shows that NGC 3680 initially contained at least $\sim$2000 stars with a total mass of $\sim$1200 $M_\odot$. Hence, only maybe 3% of the original stars and 10% of the mass now remain. Of the initial mass, $\sim$30% was in the form of $\sim$100 massive stars, potentially still observable as white dwarfs. The original $\gtrsim$90% low-mass stars, containing $\sim$60% of the mass, have escaped from the cluster field studied so far; further studies may reveal whether these stars remain in a halo around the cluster or have been lost altogether. Given the strong dynamical evolution of NGC 3680, its present-day luminosity function is not a useful diagnostic of stellar models.

*Acknowledgements.* We are grateful to M. Mayor, the late A. Duquennoy, and the rest of the CORAVEL team in Geneva for their kind help with the reduction of the radial-velocity observations. We thank B. Anthony-Twarog, J.-C. Mermilliod, P.E. Nissen, B. Twarog and

D. VandenBerg for valuable discussions and access to unpublished data. Financial support for this research from the Carlsberg Foundation, the Danish Natural Science Research Council, the Danish Board for Astronomical Research and the Smithsonian Institution (to BN and JA) is gratefully acknowledged.

## References

Aarseth S., 1996, in: Hut P., Makino J. (eds.), Dynamical Evolution of Star Clusters (IAU Symp. 174). Kluwer, Dordrecht, p. 161
Andersen J., 1991, A&AR 3, 91
Andersen J., Clausen J.V., Nordström B., Tomkin J., Mayor M., 1991, 246, 99
Andersen J., Nordström B., 1991, in: Janes K. (ed.) The Formation and Evolution of Star Clusters. ASPC 13, p. 357
Andersen J., Nordström B., Clausen J.V., 1990, ApJ 363, L33
Anthony-Twarog B.J., Heim E.A., Twarog B.A., Caldwell N., 1991, AJ 102, 1056 (AHTC)
Anthony-Twarog B.J., Mukherjee K., Caldwell N., Twarog B.A., 1988, AJ 95, 1453
Anthony-Twarog B.J., Twarog B.A., 1987, AJ 94, 1222
Anthony-Twarog B.J., Twarog B.A., McClure R.D., 1993, PASP 105, 78
Anthony-Twarog B.J., Twarog B.A., Shodhan S., 1989, AJ 98, 1634 (ATTS)
Bell R.A., 1988, AJ 95, 1484
Bell R.A., Paltoglou G., Trippico M.J., 1994, MNRAS 268, 771
Benz W., Mayor M., 1981, A&A 93, 235
Benz W., Mayor M., 1984, A&A 138, 183
Bertelli G., Bressan A., Chiosi C., 1992, ApJ 392, 522
Bertelli G., Fagotto A., Bressan A., Chiosi C., 1993, A&AS 100, 647
Bertelli G., Bressan A., Chiosi C., Fagotto A., 1994 A&AS 106, 275
Canuto V.M., Mazzitelli I., 1992, ApJ 389, 724
Carraro G., Bertelli G., Bressan A., Chiosi C., 1993, A&AS 101, 381
Carraro G., Chiosi C., 1994, A&A 287, 761
Castellani V., Chieffi A., Straniero O., 1992, ApJS 78, 517
Cayrel R., Cayrel de Strobel G., Campbell B., 1985, A&A 146, 249
Christensen-Dalsgaard J., Monteiro M.J.P.F.G., Thompson M.J., 1995, MNRAS 276, 283
Claret A., 1995, A&AS 109, 441
Claret A., Giménez A., 1992, A&AS 96, 255
Crawford D.L., Perry C.L., 1966, AJ 71, 206
Crawford D.L., Mandwewala N., 1976, PASP 88, 917
Daniel S.A., Latham D.W., Mathieu R.L., Twarog B.A., 1994, PASP 106, 281
de la Fuente Marcos R., 1995, A&A 301, 407
de la Fuente Marcos R., 1996a, A&A 308, 141
de la Fuente Marcos R., 1996b, A&A 314, 453
Demarque P., Sarajedini A., Guo X.-J., 1994, ApJ 426, 165
Dowler P., VandenBerg D.A., 1996, priv. comm. (DV96)
Duquennoy A., Mayor M., 1991, A&A 248, 485
Edvardsson B., Andersen J., Gustafsson B., Lambert D.L., Nissen P.E., Tomkin J., 1993, A&A 275, 101
Eggen O.J., 1969, ApJ 155, 439 (EG)
Eggleton, P., 1996, in: Hut P., Makino J. (eds.), Dynamical Evolution of Star Clusters (IAU Symp. 174). Kluwer, Dordrecht, p. 213
Fan X.-H., Burstein D., Chen J.-S., et al., 1996, AJ 112, 628
Friel E.D., Janes K.A., 1993, A&A 267, 75
Friel E.D., 1995, ARA&A 33, 381
Gilliland R.L., Brown T.M., Duncan D.K., et al., 1991, AJ 101, 541
Huebner W.F., Merts A.L., Magee N.H., Argo M.F., 1977, Los Alamos Sci. Lab. Rept. LA-6760-M
Iglesias C.A., Rogers F.J., Wilson B.G., 1992, ApJ 397, 717
Janes K.A., Phelps R., 1994, AJ 108, 1773
Kozhurina-Platais V., Girard T.M., Platais I., van Altena W.F., 1995, AJ 109, 672 (K95)
Kroupa P., Tout C.A., Gilmore G., 1993, MNRAS 262, 545
Leonard P.J.T., 1988, AJ 95, 108
Maeder A., Meynet G., 1989, A&A 210, 155
Mathieu R.D., Latham D.W., Griffin R.F., Gunn J.E., 1986, AJ 92, 1100
Mazzei P., Pigatto L., 1988, A&A 193, 148
Mermilliod J.-C., Andersen J., Nordström B., Mayor M., 1995, A&A 299, 53
Meynet G., Mermilliod J.-C., Maeder A., 1993, A&AS 98, 477
Miller G.E., Scalo J.M., 1979, ApJS 41, 413
Nissen P.E., 1988, A&A 199, 146 (N88)
Nissen P.E., Crawford D.L., Twarog B.A., 1987, AJ 93, 634
Nordlund Å., Stein R.F., 1996, in: Noels A., Fraipont-Caro D., Gabriel M., Grevesse N., Demarque P. (eds.), Stellar evolution: What should be done; Proc. 32nd Liège Int. Astrophys. Colloq. Univ. de Liège, Inst. d'Astrophys., Liège, p. 75
Nordström B., Andersen J., 1991, ESO Messenger 63, 34
Nordström B., Andersen J., Andersen M.I., 1996, A&AS 118, 407 (Paper I)
Olsen E.H., 1993, A&AS 102, 89
Padoan P., Nordlund Å.P., Jones B.J.T., 1996, MNRAS, in press
Paresce F., De Marchi G., Romaniello M., 1995, ApJ 440, 216
Pedersen B.B., VandenBerg D.A., Irwin A.W., 1990, ApJ, 352, 279
Rogers, F.J. Iglesias C.A., 1992, ApJS 79, 507
Roxburgh, I.W., 1978, A&A 63, 281
Roxburgh, I.W., 1992, A&A 266, 291
Salpeter, E.E., 1955, ApJ 121, 161
Saxner M., Hammarbäck G., 1985, A&A 151, 372
Schaerer D., Charbonnel C., Meynet G., Maeder A., Schaller G., 1993, A&AS 102, 339
Schaller G., Schaerer D., Meynet G., Maeder A., 1992, A&AS 96, 269 (S92)
Schwan H., 1991, A&A 243, 386
Slettebak A., 1970, in: Slettebak A. (ed.) Stellar Rotation. Reidel, Dordrecht, p. 3
Terlevich E., 1987, MNRAS 224, 193
Torres G., Stefanik R.P., Latham D.W., 1997, ApJ, in press
Twarog B.A., 1983, ApJ 267, 207
VandenBerg D.A., 1983, ApJS 51, 29
VandenBerg D.A., 1985, ApJS 58, 711
VandenBerg D.A., Bell R.A., 1985, ApJS 58, 561
VandenBerg D.A., Poll H.E., 1989, AJ 98, 1451
von Hippel T., Gilmore G., Tanvir N., Robinson D., Jones D.H.P., 1996, AJ 112, 192
Zahn J.-P., 1991, A&A 252, 179

**Note added in proof:** After the present paper was accepted, we received a preprint by Kozhurina-Platais et al. (AJ, in press), who fit solar-abundance Yale models to new *BV* photometry of NGC 3680, with results consistent with our Fig. 14.

This article was processed by the author using Springer-Verlag LaTeX A&A style file *L-AA* version 3.